MEMBRANE-ANCHORED UPAR REGULATES THE PROLIFERATION, MARROW POOL SIZE, ENGRAFTMENT AND MOBILIZATION OF HEMATOPOIETIC STEM/PROGENITOR CELLS

Marc Tjwa et al.

SUPPLEMENTAL MATERIAL

SUPPLEMENTAL RESULTS

HSPC DISTRIBUTION IN *PLAUR*$^{-/-}$ MICE

Translocation of CFU-Cs to the blood was not detected in *Plaur*$^{-/-}$ mice in steady-state conditions. The numbers of the CFU-Cs were: (i) in the BM (expressed as x 10^3 per femur): 24 ± 2 in WT mice *versus* 14 ± 1 in *Plaur*$^{-/-}$ mice (P<0.05); (ii) in the peripheral blood (expressed per ml): 60 ± 10 in WT mice *versus* 70 ± 10 *Plaur*$^{-/-}$ mice (P=NS); (iii) in the spleen (expressed per 10^5 SpMCs): 13 ± 2 in WT mice *versus* 15 ± 2 in *Plaur*$^{-/-}$ mice (P=NS). The spleen weight corrected for body weight (mg/g) was 3.7 ± 0.3 in WT mice *versus* 3.8 ± 0.3 in *Plaur*$^{-/-}$ mice.

^{M}uPAR CLEAVAGE: RATIONALE FOR THE USE OF THE 5-FU MODEL

Although G-CSF is the classical mobilizing agent, we used in these experiments 5-FU. Indeed, demonstrating that intact ^{M}uPAR expression levels are reduced on HSPCs during mobilization requires large numbers of cells. As this was technically not feasible when using the G-CSF model, we used 5-FU (200 mg/kg i.v.) to mobilize HSPCs. Apart from mobilizing HSPCs, 5-FU also eliminates lineage-positive cells from the BM leading to proliferation of lineage-negative cells (1). Hence, large numbers of Sca-1$^+$ HSPCs that are chiefly lineage-negative, can be found in the BM of animals following 5-FU administration (1). Since HSPCs loose their cKit expression during 5-FU (1), we did not analyze cKit$^+$ BMCs. However, we acknowledge the limitations of analyzing immunophenotypically different HSPC subpopulations.

FURTHER EVIDENCE FOR ^{M}uPAR CLEAVAGE DURING HSPC MOBILIZATION

^{S}uPAR levels in the BM plasma increased during mobilization in WT but not *Plg*$^{-/-}$ mice (not shown). By contrast, the MFI signal of the AK17 antibody, which recognizes all forms of ^{M}uPAR, remained unchanged on Sca-1$^+$ BMCs in WT and *Plg*$^{-/-}$ mice (p=NS; not shown), indicating the absence of genotypic differences in ^{M}uPAR expression or catabolism during mobilization.

SUPPLEMENTAL FIGURES

SUPPLEMENTAL FIGURE 1: Expression of ^{M}uPAR on HSPCs.

A, Representative FACS dot plot revealing the expression of ^{M}uPAR on Lin^{-}cKit^{+} HSPCs (*left*; isotype control: *right*). Lin^{-} BMCs were gated. ***B,*** To further assess whether *Plaur*$^{-/-}$ HSPCs home and engraft following transplantation, we co-transplanted *Plaur*$^{-/-}$ and WT donor BMMCs in lethally irradiated WT mice. To identify the transplanted donor cells, cells were harvested from WT and *Plaur*$^{-/-}$ mice, that had been intercrossed with syngeneic mice ubiquitously expressing GFP (*Actb:GFP mice*). GFP^{+} WT and *Plaur*$^{-/-}$ cells were mixed in a 3:1, 1:1, or 1:3 ratio with *Plaur*$^{-/-}$ GFP^{-} and WT GFP^{-} competitor cells, respectively, and a total of 1 x 10^{6} BMMCs were transplanted into GFP^{-} WT recipients irradiated at 8 Gy. Compared to WT GFP^{+} cells, fewer *Plaur*$^{-/-}$ GFP^{+} donor BMMCs contributed to the hematopoietic repopulation of recipient WT mice at 8 weeks after transplantation. Even when three-fold more *Plaur*$^{-/-}$ GFP^{+} BMMCs were co-transplanted with WT GFP^{-} competitor cells, only ~20% GFP^{+} cells were detected in the blood of recipient mice after 8 weeks. Of note, the reduced short-term repopulation of labeled *Plaur*$^{-/-}$ cells *versus* WT cells, when transplanted in 1:1 ratio with radioprotective cells, is consistent with the notion of a partially depleted HSPC pool in the BM of *Plaur*$^{-/-}$ mice. *: P<0.05 (N=6-10).

SUPPLEMENTAL FIGURE 2: Loss of ^{M}uPAR increases HSPC proliferation.

A,B, Representative FACS histogram plots of cell cycle analysis of WT (*A*) and *Plaur*$^{-/-}$ (*B*) Lin^{-}cKit^{+} HSPCs in steady-state conditions. ***C,*** Quantitative analysis of the cell cycle status in WT and *Plaur*$^{-/-}$ Lin^{-}cKit^{+} HSPCs in steady-state conditions. Compared to WT, fewer Lin^{-}cKit^{+} HSPCs in the BM of *Plaur*$^{-/-}$ mice were in G_0/G_1. *: P<0.05 *versus* WT (N=4). ***D,*** Compared to WT mice, fewer Lin^{-}cKit^{+} HSPCs in the *Plaur*$^{-/-}$ mice were Pyronin Y^{low}. *: P<0.05 *versus* WT (N=4). ***E,F,*** Compared to WT mice, more Lin^{-}cKit^{+} HSPCs in *Plaur*$^{-/-}$ mice proliferated (*E*) or were apoptotic (*F*). *: P<0.05 *versus* WT (N=4).

SUPPLEMENTAL FIGURE 3: Plasmin cleaves ^{M}uPAR during mobilization.

A, For plasmin to be a candidate proteinase capable of cleaving ^{M}uPAR in vivo, it should be expressed in the BM during HSPC mobilization. In normal BM, plasmin was undetectable in baseline conditions (<1 AU/ml). However, in conditions of HSPC mobilization (2 days after G-CSF), plasmin levels were transiently upregulated (*upper*; *N*=3) and declined thereafter again by day 5 to undetectable levels. At 2 days after G-CSF, the increased plasmin activity coincides with peak expansion of HSPCs in the BM (our unpublished observations). Plasmin levels were also transiently elevated in the 5-FU model on day 3 and day 7 (*lower*; *N*=3). ***B,*** Apart from cleaving ^{M}uPAR between D_I and D_{II}, plasmin also cleaves recombinant uPAR at the juxtamembrane domain (2). In doing so, plasmin induces the release of $D_ID_{II}D_{III}$ or, in case plasmin first cleaves off the D_I domain, of $D_{II}D_{III}$. ELISA measurements of intact ^{M}uPAR in total cell extracts of MDA-MB-231 cells, which express ^{M}uPAR (3), indeed showed that plasmin (administered as active plasmin or urokinase + plasminogen) lowered the amount of intact ^{M}uPAR in these cells (*N*=6; *P*<0.05). As expected, plasmin also increased the levels of ^{S}uPAR ($D_{II}D_{III}$ and $D_ID_{II}D_{III}$) in the conditioned medium of these cells (1,130 ± 200% of control levels; *N*=6; *P*<0.05). Further experiments using the domain-specific anti-uPAR antibodies revealed that plasmin also cleaves ^{M}uPAR between D_I and D_{II} (data not shown). Thus, plasmin cleaves ^{M}uPAR on intact cells in vitro.

SUPPLEMENTAL FIGURE 4: Molecular mechanisms of ^{M}uPAR

A,B, Upon adhesion of WT Lin^-cKit^+ HSPCs to immobilized sVCAM-1 (bottom of the picture), α4ß1 (green; *A*) and ^{M}uPAR (red; *B*) seemed to cluster, as revealed by multiphoton confocal microscopy (3D reconstruction). Nuclear DAPI staining is shown in blue. ***C,*** ^{M}uPAR does not cooperate with CXCR-4. Indeed, FACS analysis showed that inhibition or loss of ^{M}uPAR did not affect the expression of CXCR-4 on Lin^-cKit^+ HSPCs (not shown). To study the response of *Plaur*$^{-/-}$ HSPCs to SDF-1, we administered the CXCR-4 inhibitor AMD3100 to *Plaur*$^{-/-}$ mice and found that mobilization of CFU-Cs was comparable in WT and *Plaur*$^{-/-}$ mice (CFU-Cs x 10^3 per ml blood: 1.1 ± 0.2 in WT mice *versus* 1.0 ± 0.2 in *Plaur*$^{-/-}$ mice; N=6; P=NS). Furthermore, pre-treatment with AMD3100 modestly reduced homing of $Ly5.1^+$ Lin^-cKit^+ HSPCs to the BM, as was found previously by others (4), but, importantly, a

combination of AMD3100 plus neutralizing anti-^{M}uPAR antibodies further impaired the homing of Ly5.1^{+} Lin^{-}cKit^{+} HSPCs to the BM, indicating that both pathways operate separately. Data are expressed as % of control. For reasons of clarity and comparison, the data with anti-^{M}uPAR (Figure 3B) are shown again. *: P<0.05 *versus* control IgG; $^{\#}$: P<0.05 *versus* AMD3100 (N=4-6). ***D,*** ^{M}uPAR does not cooperate with mKitL. When performing in vitro adhesion assays with isolated Lin^{-}cKit^{+} HSPCs using mKitL-expressing BM stromal cells as substrate, inhibition or loss of ^{M}uPAR antibodies failed to inhibit cKit-mediated adhesion and FACS analysis showed that inhibition or loss of ^{M}uPAR did not affect the expression of cKit on Lin^{-}cKit^{+} HSPCs (not shown). Data in are expressed as % of control (N=8).

SUPPLEMENTAL FIGURE 5: Expression of ^{M}uPAR on KSL cells.

A, Representative FACS dot plot revealing the expression of ^{M}uPAR on KSL cells.

SUPPLEMENTAL TABLES

SUPPLEMENTAL TABLE 1: Hematopoietic profile of WT and *Plaur*$^{-/-}$ mice.

	WT mice	*Plaur*$^{-/-}$ **mice**
WBC (x 10^3/µl)	6.1 ± 0.8	7.0 ± 0.5
% neutrophils	9 ± 2	11 ± 3
% monocytes	5 ± 1	8 ± 1
% lymphocytes	86 ± 2	81 ± 3
RBC (x 10^6/µl)	8.2 ± 0.2	8.3 ± 0.2
Hct (%)	44 ± 1	46 ± 1
Reticulocytes (x 10^5/µl)	36 ± 3	31 ± 4

Values represent the mean ± SEM of the hematological parameters in WT (n=15) and *Plaur*$^{-/-}$ (n=15) mice in steady-state conditions. *P*=NS *versus* WT.

REFERENCES

1. Randall, T.D., and Weissman, I.L. 1997. Phenotypic and functional changes induced at the clonal level in hematopoietic stem cells after 5-fluorouracil treatment. *Blood* 89:3596-3606.

2. Beaufort, N., Leduc, D., Rousselle, J.C., Namane, A., Chignard, M., and Pidard, D. 2004. Plasmin cleaves the juxtamembrane domain and releases truncated species of the urokinase receptor (CD87) from human bronchial epithelial cells. *FEBS Lett* 574:89-94.

3. Holst-Hansen, C., Johannessen, B., Hoyer-Hansen, G., Romer, J., Ellis, V., and Brunner, N. 1996. Urokinase-type plasminogen activation in three human breast cancer cell lines correlates with their in vitro invasiveness. *Clin Exp Metastasis* 14:297-307.

4. Bonig, H., Priestley, G.V., and Papayannopoulou, T. 2006. Hierarchy of molecular-pathway usage in bone marrow homing and its shift by cytokines. *Blood* 107:79-86.

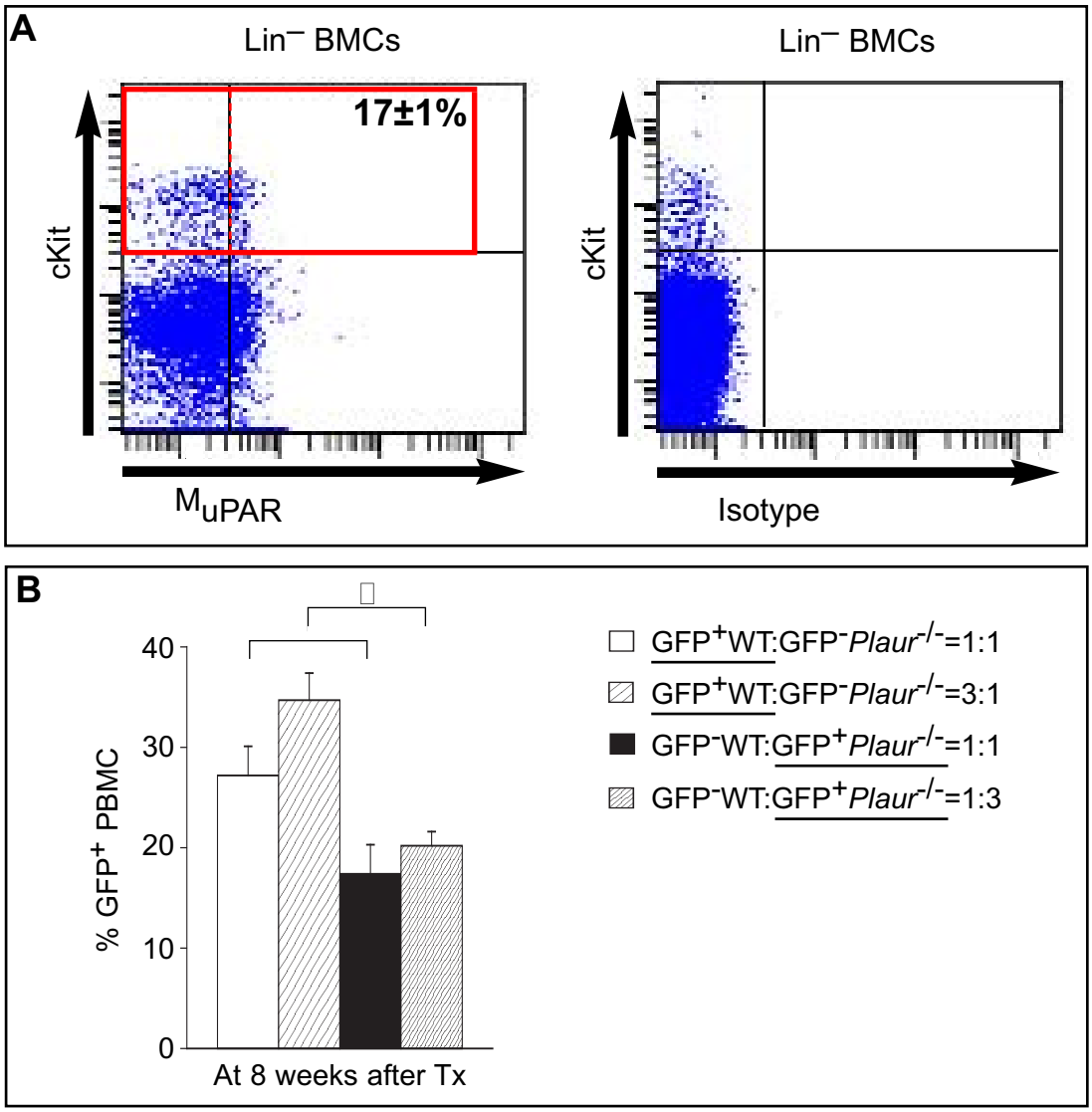

Supplemental Figure 1

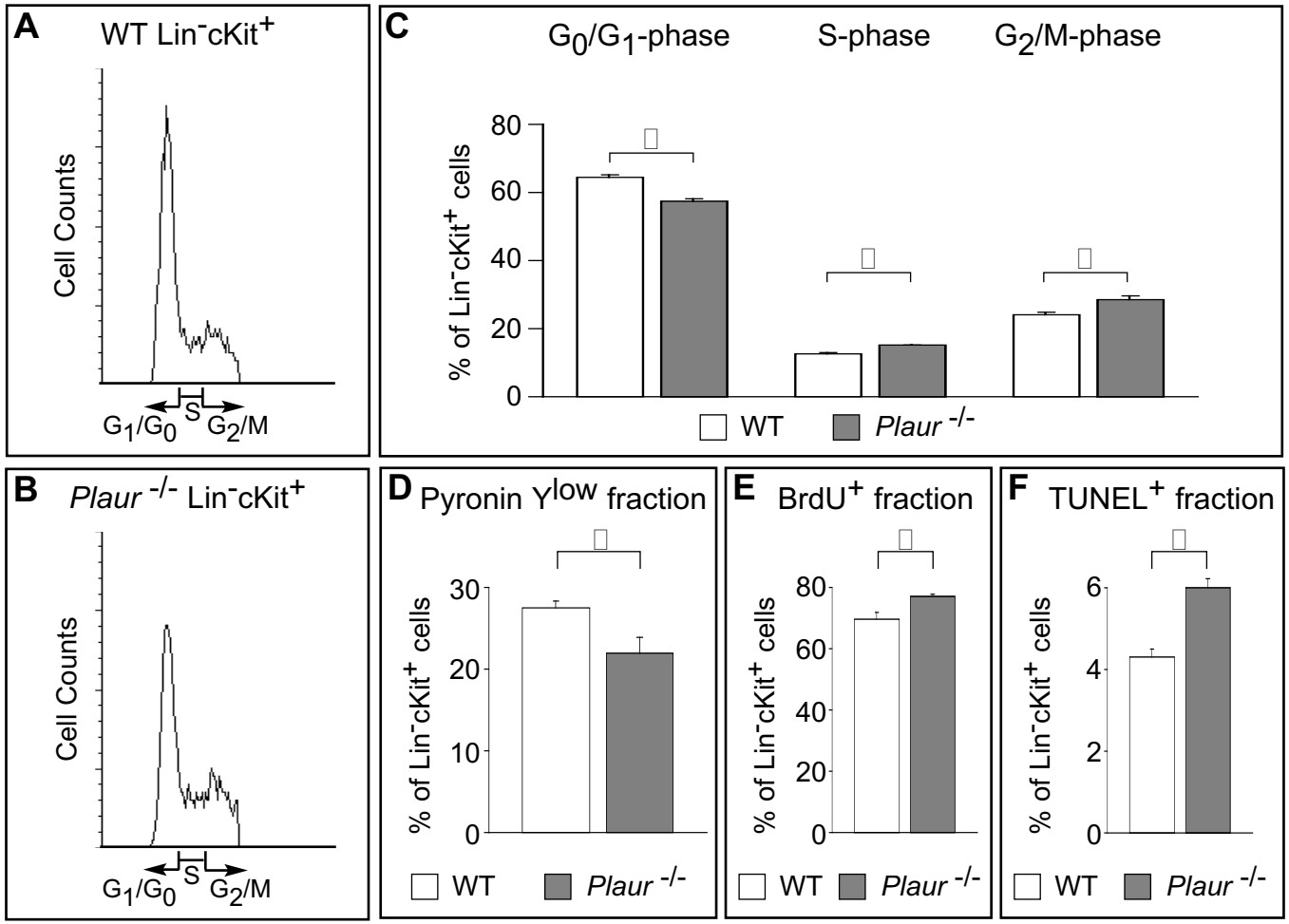

Supplemental Figure 2

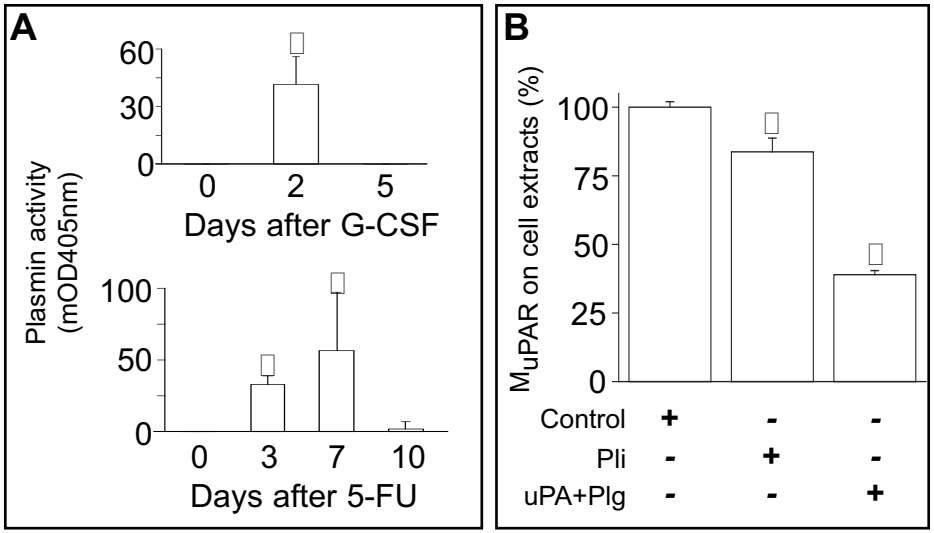

Supplemental Figure 3

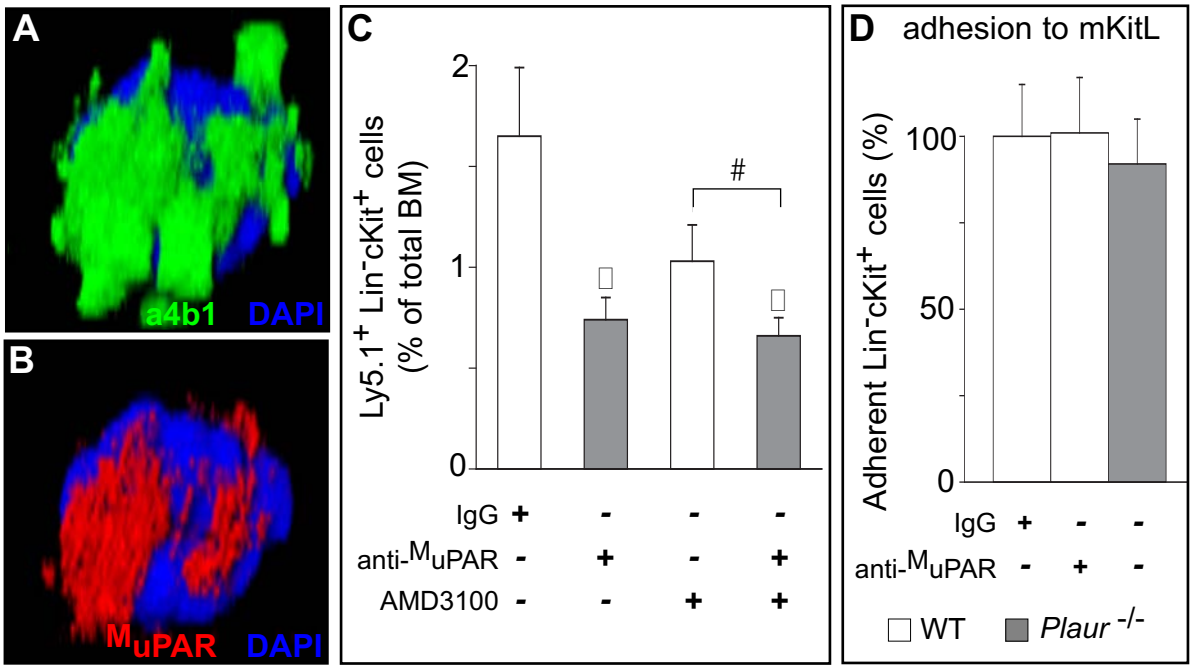

Supplemental Figure 4

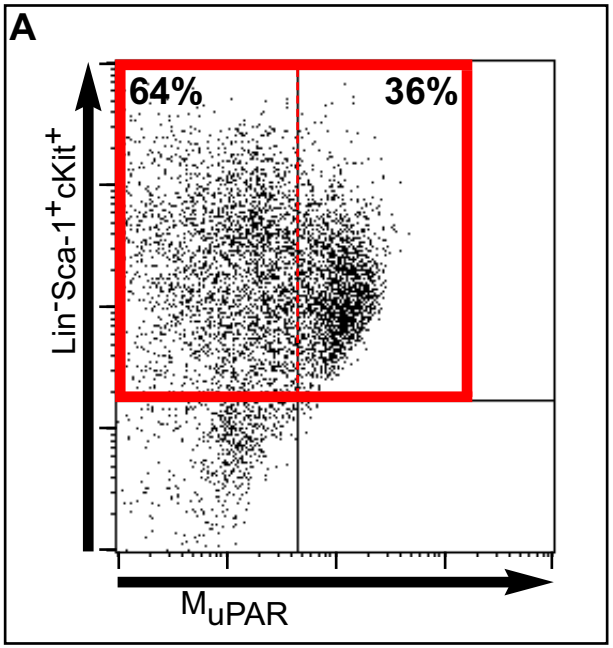

Supplemental Figure 5